

ARTICLE

Photocatalyst-free, visible-light-mediated nickel catalyzed carbon–heteroatom cross-couplings

Cristian Cavedon,^{1,2,†} Sebastian Gisbertz,^{1,2,†} Sarah Vogl,³ Noah Richter,¹ Stefanie Schrottke,⁴ Christian Teutloff,⁴ Peter H. Seeberger,^{1,2} Arne Thomas^{3*} & Bartholomäus Pieber^{1*}

¹*Department of Biomolecular Systems, Max-Planck-Institute of Colloids and Interfaces
Am Mühlenberg 1, 14476 Potsdam, Germany*

²*Department of Chemistry and Biochemistry, Freie Universität Berlin
Arnimallee 22, 14195 Berlin, Germany*

³*Department of Chemistry, Functional Materials, Technische Universität Berlin
Hardenbergstraße 40, 10623 Berlin, Germany*

⁴*Department of Physics, Freie Universität Berlin
Arnimallee 22, 14195 Berlin, Germany*

[†]*These authors contributed equally*

^{*}*Corresponding author*

Email: arne.thomas@tu-berlin.de

Email: bartholomaeus.pieber@mpikg.mpg.de

Abstract

Metallaphotocatalysis typically requires a photocatalyst to harness the energy of visible-light and transfer it to a transition metal catalyst to trigger chemical reactions. The most prominent example is the merger of photo- and nickel catalysis that unlocked various cross-couplings. However, the high reactivity of excited photocatalyst can lead to unwanted side reactions thus limiting this approach. Here we show that a bipyridine ligand that is subtly decorated with two carbazole groups forms a nickel complex that absorbs visible-light and promotes several carbon–heteroatom cross-couplings in the absence of an exogenous photocatalysts. The ligand can be polymerized in a simple one-step procedure to afford a porous organic polymer that can be used for heterogeneous nickel catalysis in the same reactions. The material can be easily recovered and reused multiple times maintaining high catalytic activity and selectivity.

38 **MAIN**

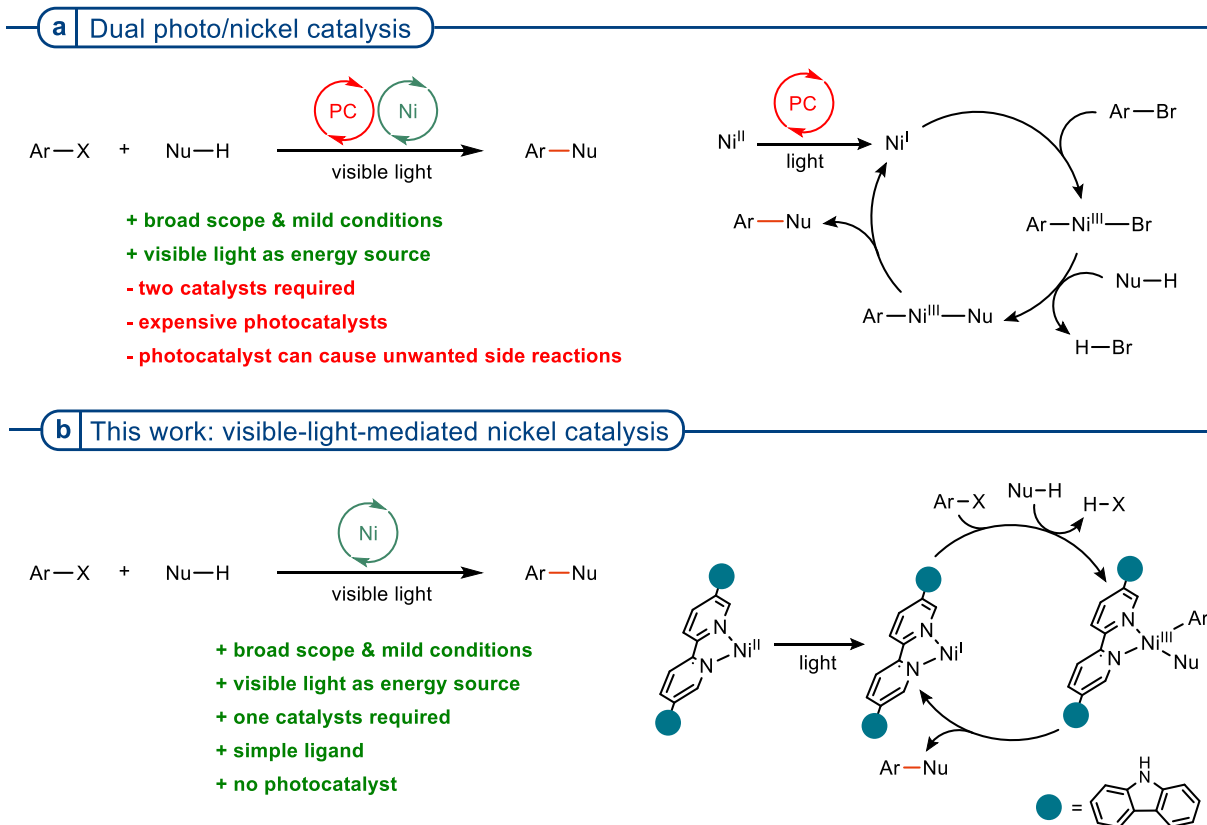
39 **Introduction**

40 Strategic carbon–carbon and carbon–heteroatom bond formations are key to the synthesis of fine
41 chemicals.^{1,2} Nickel catalysts are an abundant alternative to palladium catalysts, but reductive
42 elimination is limiting this approach.^{3,4} This problem was successfully tackled by combining nickel- and
43 photocatalysis (Fig. 1a).⁵⁻⁷ Suitable photocatalysts for dual photo/nickel catalytic carbon–heteroatom
44 cross-couplings range from ruthenium and iridium polypyridyl complexes and organic dyes to
45 heterogeneous semiconductors.⁶ Moreover, nickel complexes and visible-light photocatalysts were
46 combined in bifunctional heterogeneous materials, such as metal-organic frameworks,^{8,9} organic
47 polymers,¹⁰ or functionalized semiconductors.¹¹⁻¹⁴ Although dual photo/nickel catalysis is attractive, the
48 need for a photocatalyst is a drawback. Commonly applied homogeneous noble-metal based
49 photocatalysts that are mainly applied are expensive, not easily recyclable and unsustainable. Moreover,
50 their high reactivity upon excitation can trigger unwanted side-reactions¹⁵ and deactivation of the nickel
51 catalyst¹⁶ results in low selectivities and often poor reproducibility.

52 The first mechanistic hypothesis for dual photo/nickel catalyzed carbon–heteroatom cross-couplings
53 suggested that energy- or electron transfer between the photocatalyst and a thermodynamically stable
54 Ni^{II} intermediate triggers reductive elimination of the desired product.^{6,17} Recent studies provided
55 evidence that these reactions proceed through Ni^I/Ni^{III} cycles without a Ni^{II} resting state.¹⁸⁻²¹ Doyle and
56 colleagues showed that upon absorption of light, Ni^{II}(dtbbpy) aryl halide complexes (dtbbpy = 4,4'-di-
57 *tert*-butyl-2,2'-bipyridyl) undergo Ni–aryl hemolysis to form a catalytically active Ni^I catalyst.^{22,23} This
58 observation was expanded to a synthetic protocol for C–O and C–N cross-couplings using UV-light
59 irradiation.^{24,25} More recently, pulse radiolysis together with spectroelectrochemistry indicated that
60 Ni⁰/Ni^{II} comproportionation generates a Ni^I bipyridyl species that rapidly undergoes oxidative addition
61 with iodobenzene.²¹ Moreover, Nocera and coworkers showed that sub-stoichiometric amounts of zinc
62 can be used instead of a photocatalyst and light for C–N and C–O cross-couplings.²⁶ Here, the metal
63 reductant was proposed to generate the active Ni^I catalyst from a Ni^{II} pre-catalyst that engages in a
64 thermally sustained Ni^I/Ni^{III} cycle.

65 Based on these mechanistic findings, we questioned whether a visible-light-mediated approach to
66 nickel-catalyzed carbon–heteroatom cross-couplings without an exogenous photocatalyst or reductant
67 is feasible. The development of a benchstable Ni^{II} pre-catalyst that can be directly activated by visible-
68 light would overcome the drawbacks associated with the price and reactivity of many photocatalysts
69 without using highly energetic UV-light. We hypothesized that this can be realized via the modification
70 of a bipyridyl ligand with a structural motif that extends the absorption of an *in situ* formed Ni^{II} pre-
71 catalyst to visible-light. We speculated that such a complex might form the key Ni^I species upon
72 irradiation through, for example, homolytic fission of a Ni-halogen bond, or intramolecular charge
73 transfer.

74 Here we show that this can be indeed achieved by decorating 2-2'-bipyridine with two carbazole units
 75 (Fig. 1b). This ligand enables visible-light-mediated cross-couplings of several nucleophiles with aryl
 76 halides. Moreover, we demonstrate that the ligand can be polymerized to yield a conjugated microporous
 77 polymer that serves as a recyclable heterogeneous macroligand for metallaphotocatalytic carbon-
 78 heteroatom couplings.



79

80 **Figure 1 | Strategies for visible-light mediated nickel catalyzed carbon-heteroatom cross-**
 81 **couplings. a,** Dual photo/nickel catalysis requires a nickel catalyst and an exogenous photocatalyst. **b,**
 82 Visible-light-mediated nickel catalysis through ligand modification requires only one molecular catalyst
 83 (this work).

84 85 Ligand design and evaluation

86 Ni^{II}(dtbbpy) aryl halide complexes catalyze cross-couplings using UV-light (390 nm LEDs).^{22,23} These
 87 catalysts are synthesized from Ni(COD)₂ using glove-box or Schlenk techniques,^{22,23} which, together
 88 with the constraint to high energy photons, limits their practicability. In dual photo/nickel catalysis, on
 89 the contrary, Ni(2,2'-bipyridyl)X₂ (X = Cl, Br) complexes that form *in situ* from cheap, benchstable Ni^{II}
 90 salts and the corresponding ligand can be used.⁵⁻⁷ The UV-Vis absorption spectrum of a mixture of
 91 NiCl₂·glyme (glyme = 1,2-dimethoxyethane) and dtbbpy in DMAc (*N,N*-dimethylacetamide) shows that
 92 the resulting complex only absorbs light below 320 nm (Fig. S5). To shift the absorption towards the
 93 visible-light spectrum, we synthesized 5,5'-dicarbazolyl-2,2'-bipyridyl (czbpy) via a copper-catalyzed
 94 Ullmann coupling between 5,5'-dibromo-bipyridine and 9*H*-carbazole (Fig. 2a).²⁷ The UV-Vis
 95 spectrum of czbpy shows a strong absorption band centered at ~350 nm (Fig. S5). More importantly,

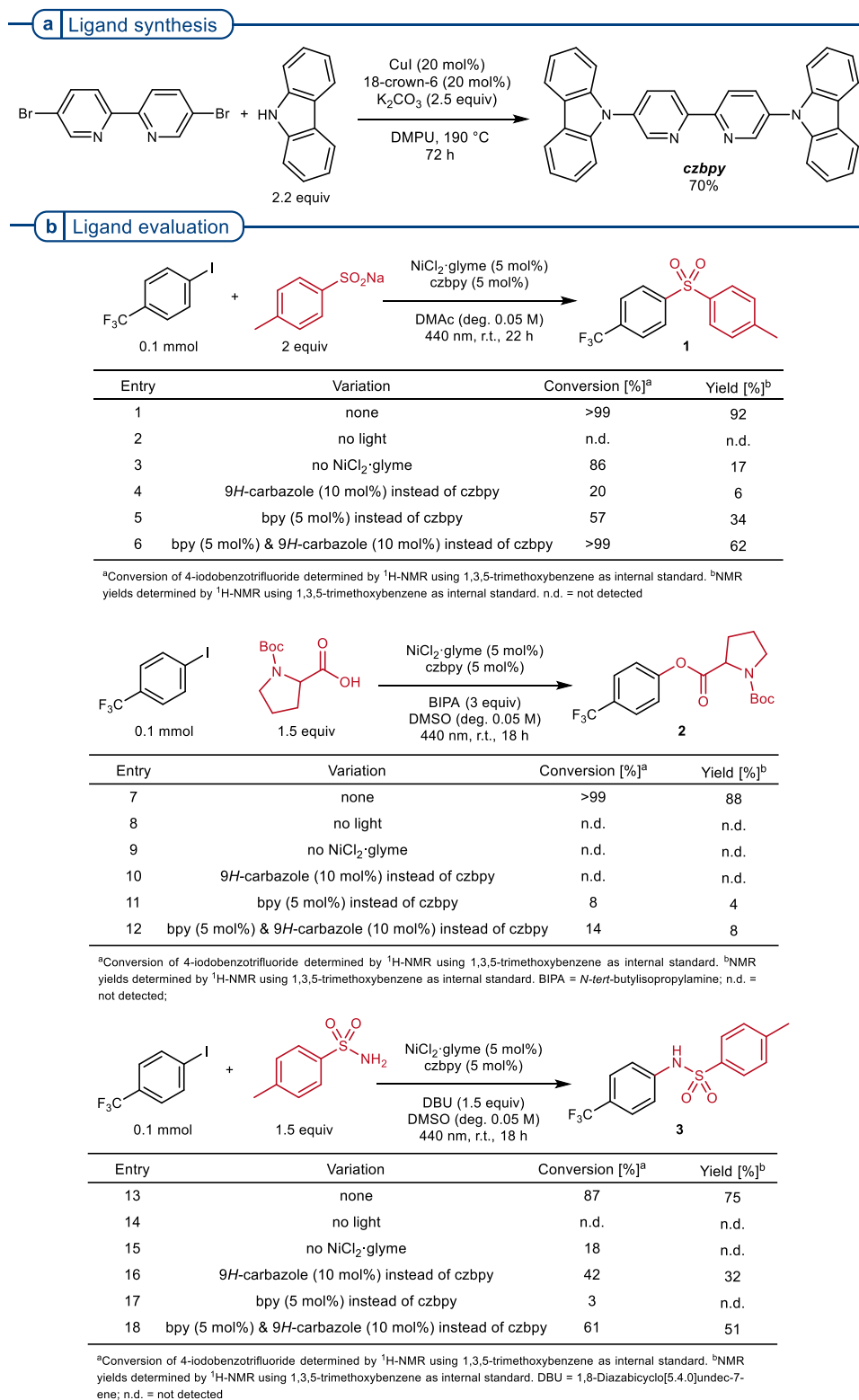
96 dissolving NiCl₂·glyme and czbpy in DMAc resulted in a complex that absorbs visible-light up to 450
97 nm (Fig. S5).

98 This single, high yielding modification of a commercially available byridine derivative resulted in an
99 in situ formed nickel catalyst that mitigates the necessity of exogenous photocatalysts (Fig. 2b). The
100 ligand was suitable for the coupling of aryl halides with sulfinates, carboxylic acids, and sulfonamides.
101 The coupling of 4-iodobenzotrifluoride and a sodium sulfinate salt (C–S coupling), which was
102 previously reported using combinations of a nickel catalyst with iridium²⁸ or ruthenium^{29,30} polypyridyl
103 complexes as photocatalyst, afforded sulfone **1** in excellent yield after 22 h irradiation with blue light
104 (440 nm, entry 1). No conversion was detected when the reaction was carried out in the dark (entry 2).
105 Sodium sulfinates and aryl halides can assemble in electron-donor acceptor (EDA) complexes and afford
106 sulfones upon UV light irradiation.³¹ Accordingly, even in absence of NiCl₂·glyme small amounts of **1**
107 were formed (entry 3), due to partial emission in the UV region of the light source. When 2,2'-bipyridine
108 (bpy), 9*H*-carbazole or a combination of bpy and 9*H*-carbazole were used, the desired product was also
109 formed, although with significantly lower selectivity (entry 4-6).

110 The C–O arylation of 4-iodobenzotrifluoride with *N*-Boc-proline under optimized conditions resulted in
111 88% of the desired product (**2**). No product formation was observed in the dark, without NiCl₂·glyme,
112 or when 9*H*-carbazole was used as ligand (entry 8-10). While optimized conditions resulted in 88% of
113 the desired product (**2**), only small amounts (<10 %) of **2** were formed using bpy, or bpy together with
114 9*H*-carbazole (entry 9, 11). These findings support our hypothesis that czbpy enables activation of nickel
115 catalysts with wavelengths above 400 nm, which are not accessible to bpy complexes.

116 Under optimized conditions, the light-mediated, nickel-catalyzed *N*-arylation of sulfonamides afforded
117 **3** in 75% yield (entry 13). Light and the nickel salt were crucial for product formation (entry 13-14).
118 Partial consumption of the starting material in the absence of a nickel salt (entry 15) might be a result
119 of a photocatalytic activation of aryl iodides.¹⁵ Product formation was not detected using bpy as ligand
120 (entry 17), but significant amounts of **3** were obtained in presence of 9*H*-carbazole (entry 16) or a
121 combination of 9*H*-carbazole and bpy (entry 16, 18). Although such reactivity was not observed in the
122 other coupling protocols, this effect might result from formation of photoactive Ni-carbazole complexes.
123 It was recently shown that carbazole acts as a strong σ -donating ligand that reduces the energy difference
124 in MLCT transitions that account for light absorption of nickel complexes.^{32,33}

125 Electron paramagnetic resonance (EPR) spectroscopy was carried out to shed some light on the reaction
126 mechanism. Up to two signals were found depending on the solution composition in frozen solution
127 (Fig. S8 & S9). The first signal with a linewidth of approx. 20 G was found in all solutions and appeared
128 to be light-independent. We assign this signal to a Cu^{II}-czbpy complex, owing to a residual Cu
129 contamination from the ligand preparation process (~ 1 mg g⁻¹ as measured by ICP-OES analysis). A
130 second, narrow signal occurred upon illumination and rapid freezing to <25 K, when at least Ni-czbpy
131 and an aryl iodide (4-iodobenzotrifluoride) were present. A kinetic analysis of a related protocol using
132 exogenous photocatalysts showed a rate dependence on the aryl halide, which was assigned to a direct



133
134
135
136
137
138
139
140

Figure 2 | Ligand synthesis, optimized reaction conditions and control experiments. a, The ligand for photocatalyst-free, visible-light-mediated nickel catalysis was synthesized via an Ullmann C–N coupling. b, Optimized Conditions and control experiments for the coupling of 4-iodobenzotrifluoride with sodium *p*-toluenesulfonate, *N*-Boc-proline and *p*-toluenesulfonamide.

141 photocatalytic activation.¹⁵ Due to its nature (microwave power saturation and linewidth), the light-
142 dependent EPR-signal is of organic origin without involvement of Ni. Therefore, we tentatively assign
143 this signal to an elusive paramagnetic species that results from a light-induced reaction between a
144 Ni-czbp species and the aryl iodide, suggesting that the aryl iodide may play a role in the activation of
145 the pre-catalyst. No signal for the proposed Ni^I intermediate was detected, which can be rationalized by
146 the instability of such three-coordinate Ni halide complexes, or rapid oxidative addition.²¹

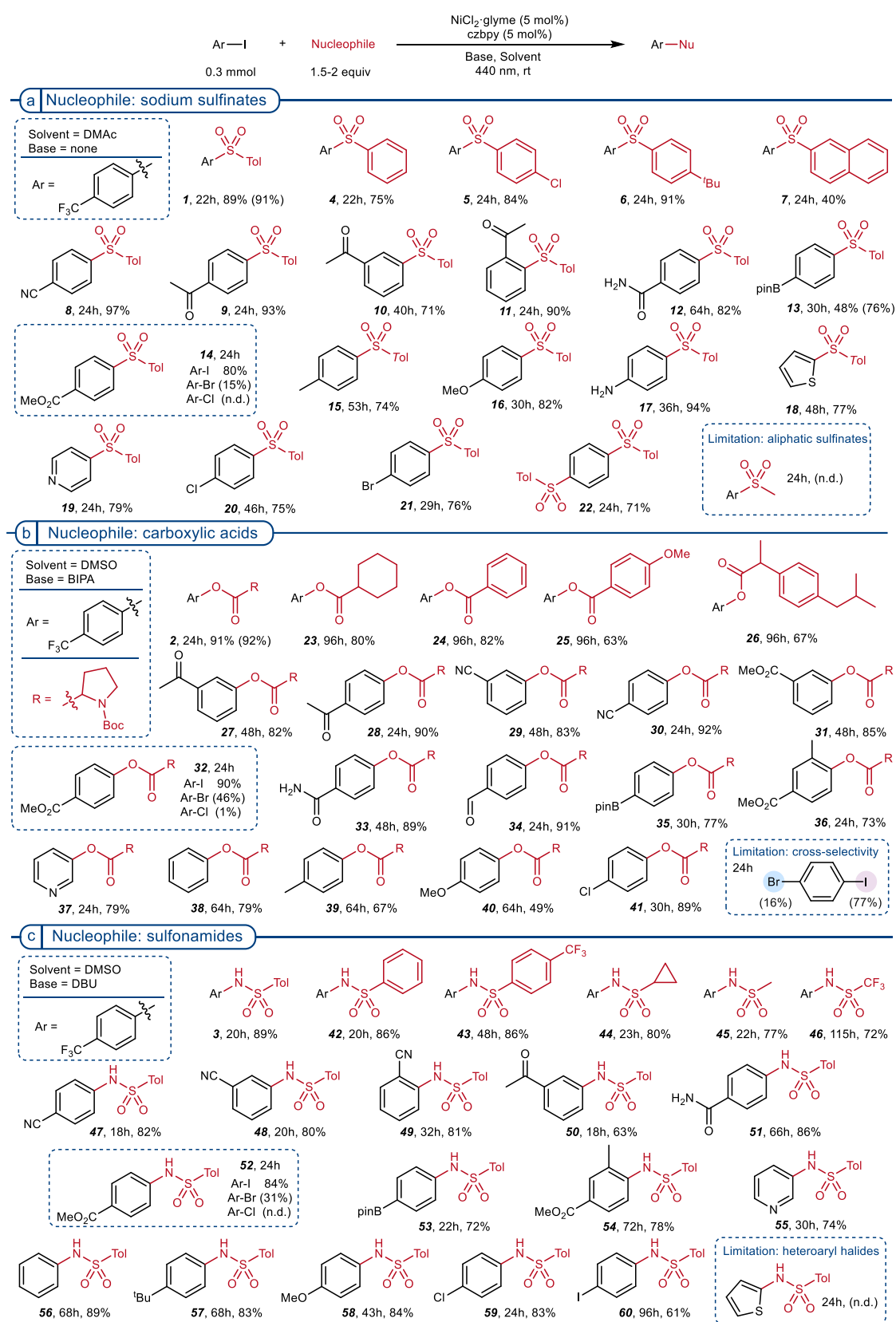
147

148 **Scope and Limitations**

149 Next, we explored the scope and limitations of photocatalyst-free, visible-light-mediated carbon-
150 heteroatom cross-couplings (Table 1). Several aromatic sulfinate salts were successfully coupled with
151 4-iodobenzotrifluoride (Table 1a, **1**, **4-7**). Optimized reaction conditions did not result in the desired
152 product using sodium methane sulfinate. It is noteworthy that this substrate was earlier reported as a
153 successful coupling partner when NiCl₂·bpy was used in combination with tris(2,2'-
154 bipyridyl)dichlororuthenium(II) hexahydrate as exogenous photocatalyst.³⁰ With regard to the aryl
155 iodide, the reaction affords the corresponding sulfones in presence of electron withdrawing groups such
156 as trifluoromethyl (**1**), nitrile (**8**), ketone (**9-11**), amide (**12**), boron pinacolate ester (**13**), and methyl
157 ester (**14**). Para- (**9**) and ortho- (**11**) substitution showed similar reactivity, whereas meta-substitution
158 (**10**) required a longer reaction time for full conversion. Electron-rich aryl iodides, such as 4-iodotoluene
159 (**15**) and 4-iodoanisole (**16**), were suitable substrates and the presence of an unprotected amine group
160 (**17**) was tolerated. Coupling of 2-iodothiophene (**18**) and 4-iodopyridine (**19**) showed that heteroaryl
161 iodides are suitable substrates.

162 A comparison of different aryl halides showed that an aryl iodide reacts significantly faster than the
163 corresponding bromide (**14**). This is in contrast to dual nickel/photocatalytic protocols, where iodides
164 and bromides exhibit similar reactivity.^{28,29} Aryl chlorides undergo nickel/photocatalytic reactions when
165 the more electron donating ligand 4,4'-dimethoxy-bpy is used,²⁸ but czbp was not suitable for aryl
166 chloride. These observations were applied for selective couplings of aryl iodides that contain a chloride
167 (**20**) or a bromide substituent (**21**). Moreover, diarylated product **22** was synthesized from 1,4-
168 diiodobenzene using three equivalents of sodium *p*-toluenesulfinate.

169 Good to excellent isolated yields were obtained for the C–O arylation of 4-iodobenzotrifluoride with
170 aliphatic and aromatic carboxylic acids (Table 1b, **2**, **23-26**). Further, a range of aryl iodides containing
171 electron-withdrawing groups afforded the corresponding products (**2**, **27-35**). The influence of the
172 substituents on the reactivity is highlighted by the longer reaction times required for the coupling of
173 meta-substituted (**27**, **29**, **31**) aryl iodides, compared to their para-substituted analogues (**28**, **30**, **32**).
174 The coupling of ortho-substituted aryl iodides was not possible in case of 2-iodoacetophenone, 2-
175 iodobenzonitrile, but **36** was successfully synthesized from methyl 3-methyl-4-iodobenzoate. A
176 heteroaryl iodide was also susceptible to the optimized reaction conditions (**38**). High electron densities
177 on the aryl iodide decreased their reactivity towards the C–O coupling, as showcased for the series 4-



179

180 ^aReaction conditions: aryl halide (300 μ mol), nucleophile (a, sodium sulfinate, 600 μ mol; b, carboxylic acid, 450 μ mol; c, sulfonamide, 450 μ mol), NiCl₂·glyme (15 μ mol), czbpy (15 μ mol), base (b, *N*-tert-butylisopropylamine, 900 μ mol; c, 1,8-diazabicyclo[5.4.0]undec-7-ene, 450 μ mol), solvent (a, DMAc, 6 mL; b, DMSO, 3 or 6 mL; c, DMSO, 6 mL), 440 nm LED (2 lamps at full power) at room temperature. Isolated yields are reported. NMR yields are in parantheses and were calculated via ¹H-NMR analysis using 1,3,5-trimethoxybenzene or maleic acid as internal standard. n.d. = not detected. Bpin = boronic acid pinacolate ester.

181

182

183

184

185 iodobenzene (**38**), 4-iodotoluene (**39**) and 4-iodoanisole (**40**). Similar to the C–S coupling described
186 above, aryl iodides work best in the reaction (**32**, 90% from Ar-I). The reaction is rather slow using the
187 corresponding bromide (46% NMR yield from Ar-Br), and a chloride afforded only traces of the desired
188 product. As a result, 1-chloro-4-iodobenzene (**41**) coupled selectively on the iodo-position, but 1-bromo-
189 4-iodobenzene reacted unselectively. All of these results are in agreement with previous reports on the
190 dual nickel/photocatalytic cross-coupling of carboxylic acids with aryl halides, indicating that the
191 photocatalyst-free strategy follows a similar mechanism.^{11,15,26,34,35}

192 Aromatic as well as aliphatic sulfonamides (**3**, **42-46**) gave selective C–N cross-couplings with 4-
193 iodobenzotrifluoride (Table 2c), even though long reaction times were necessary in case of electron-
194 withdrawing groups (**43**, **46**). In contrast to the previous C–S and C–O coupling, reactivity is not affected
195 by the substitution pattern of the aryl iodide (**47-49**, **54**) or by the presence of either electron-
196 withdrawing or electron-donating functional groups (**3**, **47-53**, **56-58**). Heteroaryl halides are
197 problematic substrates in dual nickel/photocatalytic sulfonamidation protocols and require a ligand-free
198 approach at elevated temperature.³⁶ Under our optimized conditions 3-iodopyridine gave **55** in good
199 yield, but no product was observed for 2-iodothiophene. Previously, aryl bromides were coupled with
200 sulfonamides using combinations of nickel and iridium catalysts.³⁶ Screening of different halides
201 revealed that bromides are suitable substrates but iodide reactivity is superior (**52**, 84% from Ar-I, 31%
202 NMR yield from Ar-Br within 24h). Aryl chlorides are not reactive and **59** was obtained with good
203 selectivity from 1-chloro-4-iodobenzene.

204 Unfortunately, this ligand was not suitable for coupling of aryl halides with amines, thiols or alcohols
205 that were previously reported using dual nickel/photocatalysis.⁶ Attempts to form carbon–carbon bonds
206 through coupling of aryl halides with borontrifluorides³⁷ or α -silylamines³⁸ ,also did not meet with
207 success or suffered from low selectivity (Table S30).

208

209 **Polymerization of czbpy for heterogeneous, visible-light-mediated nickel catalysis**

210 Having shown that czbpy serves as a versatile ligand for visible-light-mediated cross-couplings via
211 homogeneous nickel-catalysis without an exogenous photocatalyst, we aimed to extend this approach to
212 develop a heterogeneous, recyclable catalytic system.³⁹ Defined porous materials are ideal candidates
213 for immobilization of metal catalysts, as they enable optimal access to the catalytic sites. The
214 microporous organic polymer network poly-czbpy was synthesized from czbpy via oxidative
215 polymerization with iron(III) chloride and exhibits a Brunauer-Emmett-Teller surface area (S_{BET}) of 853
216 $\text{m}^2 \text{g}^{-1}$ (Fig. 3a).²⁷ In accordance with the literature,²⁷ the chemical structure of poly-czbpy was confirmed
217 by ^{13}C CPMAS NMR spectroscopy (Fig. S1) showing signals between 130 and 152 ppm, which verify
218 the existence of bipyridine moieties within the structure. Additionally, at 137 ppm a signal
219 corresponding to carbons in vicinity to carbazolyl nitrogen $C_{\text{Ar-N}}$ was detected. Ni@poly-czbpy was
220 subsequently prepared by refluxing a suspension of poly-czbpy and NiCl_2 in methanol. Investigation of
221 the porosity by nitrogen sorption measurements after the metalation showed a decreased BET surface

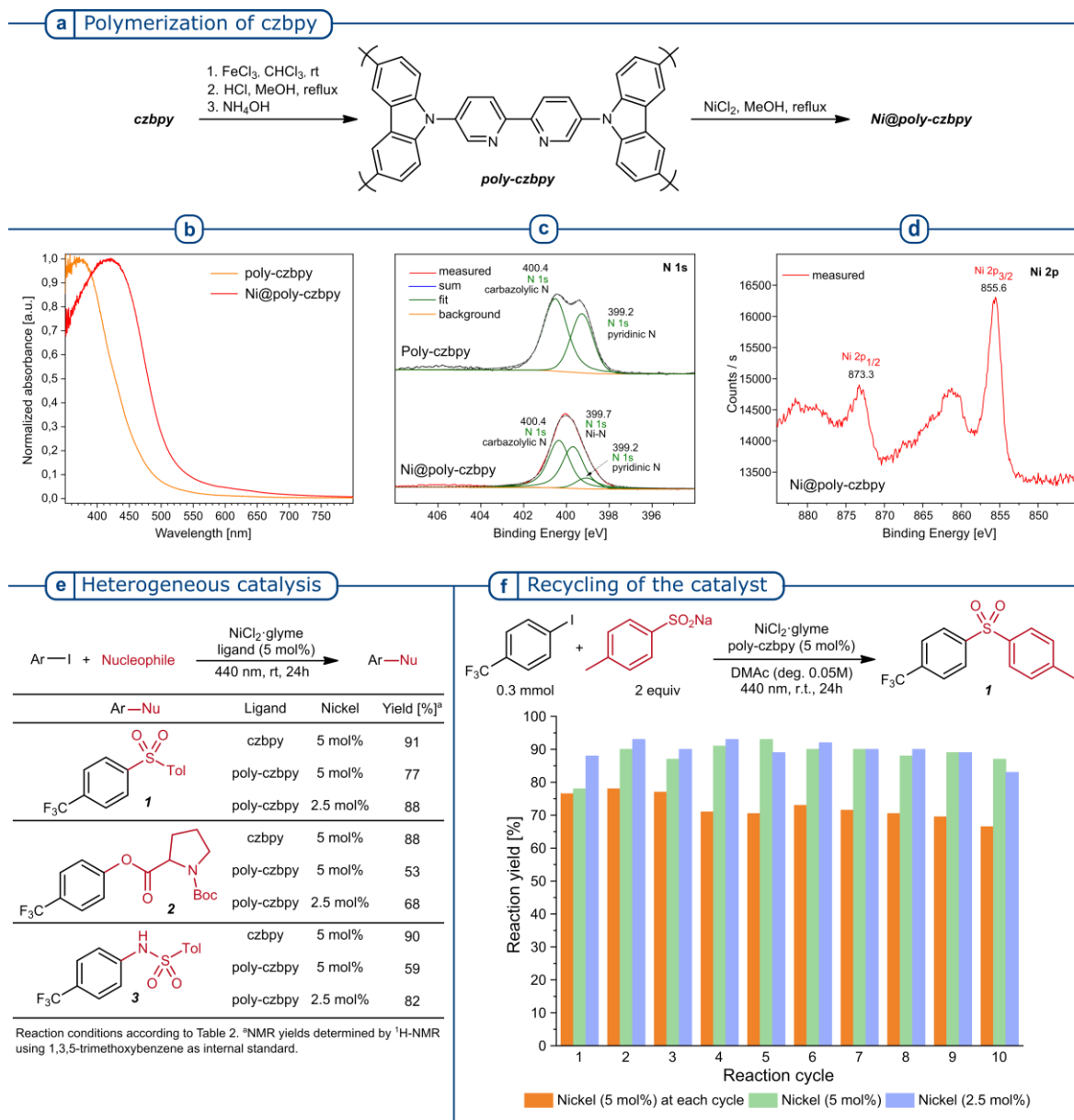
222 of 470 m² g⁻¹ due to the immobilization of the Ni(II) complex. Presence of nickel shifts the absorption
223 of the material up to 650 nm (Fig. 3b), while the metal-free ligand framework poly-czbpby absorbs until
224 550 nm. Characterization of Ni@poly-czbpby by X-ray photoelectron spectroscopy (XPS) confirmed
225 successful immobilization of Ni(II) species on the polymeric material. The N 1s core spectrum (Fig. 3c)
226 contains three signals for nitrogen: i) an intense peak at 400.4 eV corresponding to polymerized
227 carbazole moieties, ii) a signal at 399.7 eV which is assigned to N-Ni coordination of the Ni(II)-complex
228 and iii) a low-intensity peak at 400.2 eV deriving from bipyridine nitrogen species which are not
229 coordinated to nickel. The Ni 2p spectrum (Fig. 3d) shows a doublet and its corresponding satellites.
230 Peaks located at 855.6 eV and 873.3 eV are assigned to 2p_{3/2} and 2p_{1/2} signals for Ni(II) species,
231 respectively. ICP-OES analysis indicated presence of 3.7% w/w of nickel on the material Ni@poly-
232 czbpby, corresponding to an occupation of 40% of bipyridine functionalities. Furthermore, scanning
233 electron microscopy (SEM) images of Ni@poly-czbpby show the morphology of the amorphous
234 polymeric particles analyzed by elemental mapping (Fig. S2). The images depict a homogeneous
235 distribution of nickel, nitrogen and chlorine within the material.

236 After confirming that poly-czbpby is suitable to coordinate and immobilize nickel atoms, its use in the
237 previously optimized coupling reactions was studied (Fig. 3e). The desired C-S, C-O and C-N coupling
238 products were obtained by irradiation at 440 nm of mixtures of NiCl₂·glyme (5 mol%) and poly-czbpby
239 (5 mol%), but the selectivity of the reactions was lower than using homogeneous conditions.

240 Next, we studied whether the heterogeneous catalytic system based on poly-czbpby can be recycled. Poly-
241 czbpby was recovered after the C-S coupling reaction by centrifugation and was, after washing, reused
242 for the same reaction (Fig. 3f). Initial results confirmed that poly-czbpby can be recycled ten times
243 without significant loss in reactivity (orange bars). The addition of the nickel salt at each reaction cycle
244 was not necessary in a second set of experiments (green bars) and the selectivity of the reaction improved
245 upon washing and reusing the material without addition of fresh nickel salt (1st cycle: 78% yield, 2nd
246 cycle: 90% yield). According to ICP-OES analysis, 40% of the pyridine sites in poly-czbpby coordinate
247 to nickel. Therefore, equimolar amounts of nickel and poly-czbpby lead to an excess of unligated nickel
248 in solution that presumably has a detrimental effect on the selectivity. This was confirmed during a
249 series of experiments using lower nickel salt/macroligand ratio (2.5 mol% of NiCl₂·glyme, 5 mol% poly-
250 czbpby) that improved selectivity for all transformations (Table S22-S24). A final recycling experiment
251 where 2.5 mol% of NiCl₂·glyme was loaded only for the first reaction (Fig. 3f, blue bars) resulted in
252 excellent yields for the C-S coupling reaction without significant loss in activity during ten recycling
253 experiments.

254 The 2p Ni XPS spectra (Fig. S6) of the recycled catalyst confirm that the Ni(II) species remained intact
255 within the polymer network demonstrating the recyclability of the material. The signals for the doublet
256 were detected at 856.6 eV (2p_{3/2}) and 874.6 eV (2p_{1/2}), respectively. Furthermore, 1s N XPS core-level
257 spectra (Fig. S7) show that by single addition of Ni(II) precursor predominantly the pyridinic nitrogen

258 signal at 399.2 eV was detected due to relatively low amount of Ni(II) coordinated to bipyridine, while
 259 addition of Ni(II) after each cycle result mainly in Ni-N coordination signals at 399.7 eV.
 260
 261



262
 263
 264 **Figure 3 | Heterogeneous visible-light-mediated nickel catalysis with poly-czbpy.**
 265 **a**, Preparation of the porous organic polymer poly-czbpy and metalation with nickel. **b**, Characterization of poly-
 266 czbpy and Ni@poly-czbpy by UV-visible spectroscopy. XPS analysis of Ni@poly-czbpy: N 1s (**c**) and Ni 2p core-level
 267 spectra (**d**). **e**, Heterogeneous visible-light-mediated nickel catalysis using poly-czbpy. **f**, Catalyst recycling in the
 268 C-S coupling reaction. Reaction conditions: 4-iodobenzotrifluoride (300 μmol), sodium *p*-toluenesulfonate (600
 269 μmol), NiCl₂·glyme (7.5-15 μmol), poly-czbpy (7.43 mg), DMAc (6 mL), 440 nm LED (two lamps at full power)
 270 at room temperature. Yields were calculated via ¹H-NMR analysis using 1,3,5-trimethoxybenzene as internal
 271 standard. Orange: 5 mol% of NiCl₂·glyme at each reaction cycle; green: 5 mol% of NiCl₂·glyme only for the first
 272 cycle; blue: 2.5 mol% of NiCl₂·glyme only for the first cycle.
 273
 274
 275

276 **Conclusion**

277 Combining a Ni(II) salt with czbpy results in a homogeneous complex that absorbs up to 450 nm and
278 enables visible-light-mediated carbon–heteroatom cross-couplings without exogenous photocatalysts.
279 Selective C–S, C–O and C–N bond formations were achieved by coupling aryl iodides with sodium
280 sulfonates, carboxylic acids or sulfonamides, respectively. A porous organic polymer that was prepared
281 by oxidative polymerization of czbpy, is suitable for immobilization of nickel and enables
282 heterogeneous, visible-light-mediated nickel catalysis. The heterogeneous material recovered after the
283 reaction can be reused, maintaining a high activity over ten reaction cycles. EPR experiments indicated
284 an involvement of the aryl iodide for the light-mediated activation of the pre-catalyst. Further
285 investigations to understand the mechanism of these reactions are currently underway in our laboratory.
286

287 **Methods**

288 **Experimental procedure for the synthesis of 5,5'-Di(9H-carbazol-9-yl)-2,2'-bipyridine** 289 **(czbpy).**

290 Under Argon atmosphere, a mixture of 5,5'-dibromo-2,2'-bipyridine (500 mg, 1.59 mmol), carbazole
291 (586 mg, 3.5 mmol), copper(I) iodide (61 mg, 0.32 mmol), 18-crown-6 (84 mg, 0.32 mmol), potassium
292 carbonate (549 mg, 3.98 mmol) and 1,3-dimethyl-3,4,5,6-tetrahydro-2(1H)-pyrimidinone (DMPU, 1.67
293 mL) were placed in a pre-heated 100 mL Schlenk flask. The flask was connected to a reflux condenser
294 before the mixture was stirred for 24 h at 190 °C in an oil bath. At 190 °C the reaction mixture turned
295 into a yellow solution, after 24 h a black viscous oil was obtained which was quenched with 2 M HCl
296 solution (100 mL). The mixture was extracted with dichloromethane and washed with NH₃·H₂O (25%,
297 60 mL) and water. The combined organic layers were dried over magnesium sulfate and the solvent was
298 removed in vacuo. The crude product was purified by column chromatography on amino-functionalized
299 silica gel from cyclohexane and dichloromethane. The obtained yellow solid was further purified by
300 recrystallization from a mixture of cyclohexane and dichloromethane to afford the title compound as a
301 light yellow crystalline solid (540 mg, 1.11 mmol, 70 %).

302 ¹H NMR (400 MHz, CDCl₃) δ 9.03 (d, J = 1.8 Hz, 2H), 8.81 (d, J = 7.7 Hz, 2H), 8.19 (d, J = 7.7 Hz,
303 4H), 8.15 (dd, J = 8.4, 2.6 Hz, 2H), 7.55 – 7.44 (m, 8H), 7.36 (m, 4H). ¹³C NMR (101 MHz, CDCl₃) δ
304 153.5, 147.5, 140.6, 135.5, 135.2, 126.6, 124.0, 122.5, 121.0, 120.8, 109.6. HRMS (ESI) m/z calcd for
305 C₃₄H₂₃N₄ [(M+H)⁺] 487.1923, found 487.1918. This data is in full agreement with the data previously
306 published in the literature.^{27,40}

307

308 **Poly-czbpy was prepared by polymerization of czbpy according to literature.²⁷**

309 5,5'-Di(9H-carbazol-9-yl)-2,2'-bipyridine (200 mg, 0.41 mmol) was dissolved in anhydrous chloroform
310 (30 mL) and added dropwise to a suspension of FeCl₃ (1.20 g, 7.40 mmol) in anhydrous chloroform (30
311 mL) under argon. The reaction mixture was stirred at room temperature for 24 h. Then methanol (50

312 mL) was added, and the mixture was stirred vigorously for 2 h. The insoluble solid was collected by
313 filtration and washed with tetrahydrofuran and chloroform, respectively. The filtration cake was
314 transferred into a solution of HCl in methanol (6 M, 50 mL) and heated for 48 h under agitation. The
315 methanolic HCl solution was replaced by a fresh one every 24 h. The precipitate was filtered and
316 subsequently washed with aqueous ammonia solution (10 wt %) and methanol, respectively. The
317 resulting solid was finally purified through Soxhlet extraction in methanol and dried in vacuo at 80 °C
318 for 12 h to afford poly-czbpy as a yellow powder (190 mg, 95%).

319

320 **Experimental procedure for homogeneous visible-light-mediated nickel catalysis**

321 An oven dried vial (19 x 100 mm) equipped with a stir bar was charged with NiCl₂·glyme (3.3 mg, 15
322 μmol, 5 mol%), czbpy (7.3 mg, 15 μmol, 5 mol%), the aryl iodide (300 μmol) and the nucleophile (C–
323 S: sodium sulfinate, 600 μmol, equiv; C–O: carboxylic acid, 450 μmol, 1.5 equiv; C–N: sulfonamide,
324 450 μmol, 1.5 equiv). Solvent (C–S: DMAc, 6mL; C–O: DMSO, 3 mL; C–N: DMSO, 6 mL) and base
325 (C–O: N-tert-butylisopropylamine, 900 μmol, 3 equiv; C–N: 1,8-diazabicyclo[5.4.0]undec-7-ene, 450
326 μmol, 1.5 equiv) were added, then the vessel was sealed with a septum and Parafilm. The mixture was
327 stirred for 1 minute at high speed, followed by sonication for 5 minutes and degassing by bubbling argon
328 for 10 minutes. The reaction mixture was stirred at high speed (800 rpm) while irradiating it with two
329 LED lamps (440 nm) at full power. After the respective reaction time, an internal standard (maleic acid
330 34.9 mg, 300 μmol, 1 equiv or 1,3,5-trimethoxybenzene 50.5 mg, 300 μmol, 1 equiv) was added to the
331 reaction vessel, the mixture was stirred and an aliquote (20 μL) was diluted in DMSO-*d*₆ and analyzed
332 by ¹H-NMR. The NMR sample and the reaction mixture were combined together and diluted (C–S:
333 0.5M HCl, 60 mL; C–O: water, 40 mL; C–N: water, 60 mL). The aqueous phase was extracted (C–S
334 and C–N: ethyl acetate, 3x40 mL; C–O: DCM, 3x40 mL). Collected organic layers were washed with
335 brine (2 x 40 mL) and dried on Na₂SO₄ before removing solvents under reduced pressure. The residue
336 was purified by flash chromatography on silica gel using mixtures of hexane/ethyl acetate to obtain the
337 desired product.

338

339 **Experimental procedure for heterogeneous visible-light-mediated nickel catalysis**

340 An oven dried vial (13 x 80 mm) equipped with a stir bar was charged with poly-czbpy (7.3 mg), sodium
341 *p*-toluensulfinate (106.9 mg, 0.6 mmol, 2 equiv.) and NiCl₂·glyme (3.3 mg, 15 μmol, 5 mol%).
342 Subsequently, 4-iodobenzotrifluoride (81.6 mg, 0.3 mmol, 1 equiv.) and DMAc (anhydrous, 6 mL) were
343 added and the vial was sealed with a septum and Parafilm. The reaction mixture was sonicated for 5-10
344 min followed by stirring for 5 min until fine dispersion of the solids was achieved and the mixture was
345 then degassed by bubbling N₂ for 10 min. The mixture was stirred at high speed (800 rpm) while
346 irradiating it with two blue LED lamps (440 nm) at full power. After the respective reaction time, one
347 equivalent of 1,3,5-trimethoxybenzene (50.5 mg, 0.3 mmol) was added and the mixture was stirred for

348 5 min. The reaction mixture was centrifuged at 3500 rpm for 15 min and the liquid phase was carefully
349 separated and analyzed by ¹H-NMR. The recovered poly-czbpby was washed two times with DMAc
350 (anhydrous, 6 mL, followed by centrifugation at 3500 rpm for 15 min and separation of the liquid phase),
351 lyophilized (overnight) and reused in the next reaction.

352

353 **Data availability**

354 All experimental procedures and analytical data are available in the Supplementary Information. All
355 data is available from the authors on reasonable request.

356

357 **References**

- 358 1 Biffis, A., Centomo, P., Del Zotto, A. & Zecca, M. Pd Metal Catalysts for Cross-Couplings
359 and Related Reactions in the 21st Century: A Critical Review. *Chem. Rev.* **118**, 2249-2295,
360 (2018).
- 361 2 Ruiz-Castillo, P. & Buchwald, S. L. Applications of Palladium-Catalyzed C-N Cross-
362 Coupling Reactions. *Chem. Rev.* **116**, 12564-12649, (2016).
- 363 3 Tasker, S. Z., Standley, E. A. & Jamison, T. F. Recent advances in homogeneous nickel
364 catalysis. *Nature* **509**, 299-309, (2014).
- 365 4 Ananikov, V. P. Nickel: The "Spirited Horse" of Transition Metal Catalysis. *ACS Catal.* **5**,
366 1964-1971, (2015).
- 367 5 Twilton, J. *et al.* The merger of transition metal and photocatalysis. *Nat. Rev. Chem.* **1**, 0052,
368 (2017).
- 369 6 Zhu, C., Yue, H., Jia, J. & Rueping, M. Nickel-Catalyzed C-Heteroatom Cross-Coupling
370 Reactions under Mild Conditions via Facilitated Reductive Elimination. *Angew. Chem. Int.*
371 *Ed.*, <https://doi.org/10.1002/anie.202013852>, (2021).
- 372 7 Cavedon, C., Seeberger, P. H. & Pieber, B. Photochemical Strategies for Carbon-Heteroatom
373 Bond Formation. *Eur. J. Org. Chem.* **2020**, 1379-1392, (2019).
- 374 8 Lan, G. *et al.* Metal-Organic Layers as Multifunctional Two-Dimensional Nanomaterials for
375 Enhanced Photoredox Catalysis. *J. Am. Chem. Soc.* **141**, 15767-15772, (2019).
- 376 9 Zhu, Y. Y. *et al.* Merging Photoredox and Organometallic Catalysts in a Metal-Organic
377 Framework Significantly Boosts Photocatalytic Activities. *Angew. Chem. Int. Ed.* **57**, 14090-
378 14094, (2018).
- 379 10 Pan, Y. *et al.* Boosting Photocatalytic Activities for Organic Transformations through
380 Merging Photocatalyst and Transition-Metal Catalyst in Flexible Polymers. *ACS Catal.* **10**,
381 11758-11767, (2020).
- 382 11 Reischauer, S., Strauss, V. & Pieber, B. Modular, Self-Assembling Metallaphotocatalyst for
383 Cross-Couplings Using the Full Visible-Light Spectrum. *ACS Catal.* **10**, 13269-13274, (2020).
- 384 12 Vijeta, A., Casadevall, C., Roy, S. & Reisner, E. Visible-Light Promoted C-O Bond
385 Formation with an Integrated Carbon Nitride-Nickel Heterogeneous Photocatalyst. *Angew.*
386 *Chem. Int. Ed.* **60**, 8494-8499, (2021).
- 387 13 Zhao, X. *et al.* Nickel-Coordinated Carbon Nitride as a Metallaphotoredox Platform for the
388 Cross-Coupling of Aryl Halides with Alcohols. *ACS Catal.* **10**, 15178-15185, (2020).
- 389 14 Reischauer, S. & Pieber, B. Recyclable, Bifunctional Metallaphotocatalysts for C-S Cross-
390 Coupling Reactions. *ChemPhotoChem*, <https://doi.org/10.1002/cptc.202100062>, (2021).
- 391 15 Malik, J. A., Madani, A., Pieber, B. & Seeberger, P. H. Evidence for Photocatalyst
392 Involvement in Oxidative Additions of Nickel-Catalyzed Carboxylate O-Arylations. *J. Am.*
393 *Chem. Soc.* **142**, 11042-11049, (2020).
- 394 16 Gisbertz, S., Reischauer, S. & Pieber, B. Overcoming limitations in dual photoredox/nickel-
395 catalysed C-N cross-couplings due to catalyst deactivation. *Nat. Catal.* **3**, 611-620, (2020).
- 396 17 Qi, Z. H. & Ma, J. Dual Role of a Photocatalyst: Generation of Ni(0) Catalyst and Promotion
397 of Catalytic C-N Bond Formation. *ACS Catal.* **8**, 1456-1463, (2018).

- 398 18 Qin, Y., Sun, R., Gianoulis, N. P. & Nocera, D. G. Photoredox Nickel-Catalyzed C-S Cross-
399 Coupling: Mechanism, Kinetics, and Generalization. *J. Am. Chem. Soc.* **143**, 2005-2015,
400 (2021).
- 401 19 Till, N. A., Tian, L., Dong, Z., Scholes, G. D. & MacMillan, D. W. C. Mechanistic Analysis
402 of Metallaphotoredox C-N Coupling: Photocatalysis Initiates and Perpetuates Ni(I)/Ni(III)
403 Coupling Activity. *J. Am. Chem. Soc.* **142**, 15830-15841, (2020).
- 404 20 Sun, R. *et al.* Elucidation of a Redox-Mediated Reaction Cycle for Nickel-Catalyzed Cross
405 Coupling. *J. Am. Chem. Soc.* **141**, 89-93, (2019).
- 406 21 Till, N. A., Oh, S., MacMillan, D. W. C. & Bird, M. J. The Application of Pulse Radiolysis to
407 the Study of Ni(I) Intermediates in Ni-Catalyzed Cross-Coupling Reactions. *J. Am. Chem.*
408 *Soc.* **143**, 9332-9337, (2021).
- 409 22 Ting, S. I. *et al.* (3)d-d Excited States of Ni(II) Complexes Relevant to Photoredox Catalysis:
410 Spectroscopic Identification and Mechanistic Implications. *J. Am. Chem. Soc.* **142**, 5800-5810,
411 (2020).
- 412 23 Shields, B. J., Kudisch, B., Scholes, G. D. & Doyle, A. G. Long-Lived Charge-Transfer States
413 of Nickel(II) Aryl Halide Complexes Facilitate Bimolecular Photoinduced Electron Transfer.
414 *J. Am. Chem. Soc.* **140**, 3035-3039, (2018).
- 415 24 Li, G. *et al.* Light-Promoted C-N Coupling of Aryl Halides with Nitroarenes. *Angew. Chem.*
416 *Int. Ed.* **60**, 5230-5234, (2021).
- 417 25 Yang, L. *et al.* Light-Promoted Nickel Catalysis: Etherification of Aryl Electrophiles with
418 Alcohols Catalyzed by a Ni(II) -Aryl Complex. *Angew. Chem. Int. Ed.* **59**, 12714-12719,
419 (2020).
- 420 26 Sun, R., Qin, Y. & Nocera, D. G. General Paradigm in Photoredox Nickel-Catalyzed Cross-
421 Coupling Allows for Light-Free Access to Reactivity. *Angew. Chem. Int. Ed.* **59**, 9527-9533,
422 (2020).
- 423 27 Liang, H. P. *et al.* Rhenium-Metalated Polypyridine-Based Porous Polycarbazoles for Visible-
424 Light CO₂ Photoreduction. *ACS Catal.* **9**, 3959-3968, (2019).
- 425 28 Yue, H., Zhu, C. & Rueping, M. Cross-Coupling of Sodium Sulfinates with Aryl, Heteroaryl,
426 and Vinyl Halides by Nickel/Photoredox Dual Catalysis. *Angew. Chem. Int. Ed.* **57**, 1371-
427 1375, (2018).
- 428 29 Cabrera-Afonso, M. J. *et al.* Engaging sulfinate salts via Ni/photoredox dual catalysis enables
429 facile Csp²-SO₂R coupling. *Chem. Sci.* **9**, 3186-3191, (2018).
- 430 30 Liu, N. W., Hofman, K., Herbert, A. & Manolikakes, G. Visible-Light Photoredox/Nickel
431 Dual Catalysis for the Cross-Coupling of Sulfinic Acid Salts with Aryl Iodides. *Org. Lett.* **20**,
432 760-763, (2018).
- 433 31 Chen, L. *et al.* A Convenient Synthesis of Sulfones via Light Promoted Coupling of Sodium
434 Sulfinates and Aryl Halides. *Adv. Synth. Catal.* **361**, 956-960, (2019).
- 435 32 Wong, Y. S., Tang, M. C., Ng, M. & Yam, V. W. Toward the Design of Phosphorescent
436 Emitters of Cyclometalated Earth-Abundant Nickel(II) and Their Supramolecular Study. *J.*
437 *Am. Chem. Soc.* **142**, 7638-7646, (2020).
- 438 33 Alrefai, R., Hörner, G., Schubert, H. & Berkefeld, A. Broadly versus Barely Variable
439 Complex Chromophores of Planar Nickel(II) from κ^3 -N,N',C and κ^3 -N,N',O Donor
440 Platforms. *Organometallics* **40**, 1163-1177, (2021).
- 441 34 Pieber, B. *et al.* Semi-heterogeneous Dual Nickel/Photocatalysis using Carbon Nitrides:
442 Esterification of Carboxylic Acids with Aryl Halides. *Angew. Chem. Int. Ed.* **58**, 9575-9580,
443 (2019).
- 444 35 Welin, E. R., Le, C., Arias-Rotondo, D. M., McCusker, J. K. & MacMillan, D. W.
445 Photosensitized, energy transfer-mediated organometallic catalysis through electronically
446 excited nickel(II). *Science* **355**, 380-385, (2017).
- 447 36 Kim, T., McCarver, S. J., Lee, C. & MacMillan, D. W. C. Sulfonamidation of Aryl and
448 Heteroaryl Halides through Photosensitized Nickel Catalysis. *Angew. Chem. Int. Ed.* **57**, 3488-
449 3492, (2018).
- 450 37 Tellis, J. C., Primer, D. N. & Molander, G. A. Dual catalysis. Single-electron transmetalation
451 in organoboron cross-coupling by photoredox/nickel dual catalysis. *Science* **345**, 433-436,
452 (2014).

- 453 38 Remeur, C., Kelly, C. B., Patel, N. R. & Molander, G. A. Aminomethylation of Aryl Halides
454 using alpha-Silylamines Enabled by Ni/Photoredox Dual Catalysis. *ACS Catal.* **7**, 6065-6069,
455 (2017).
- 456 39 Gisbertz, S. & Pieber, B. Heterogeneous Photocatalysis in Organic Synthesis.
457 *ChemPhotoChem* **4**, 456-475, (2020).
- 458 40 Li, H.-Y. *et al.* Synthesis, structural characterization and photoluminescence properties of
459 rhenium(I) complexes based on bipyridine derivatives with carbazole moieties. *Dalton Trans.*
460 **47** 10563-10569, (2009).

461

462 **Acknowledgments**

463 C.C., S.G., N.R., P.H.S, and B.P. gratefully acknowledge the Max-Planck Society for generous financial
464 support. S.G. and B.P. thank the International Max Planck Research School on Multiscale Bio-Systems
465 for funding. B.P. acknowledge financial support by a Liebig Fellowship of the German Chemical
466 Industry Fund (Fonds der Chemischen Industrie, FCI). B.P. and A.T. thank the Deutsche
467 Forschungsgemeinschaft (DFG, German Research Foundation) under Germany's Excellence Strategy –
468 EXC 2008 – 390540038 – UniSysCat and S.V. the project TH 1463/15-1 for financial support. We thank
469 Prof. R. Bittl and Dr. John J. Molloy for scientific support and fruitful discussions.

470

471 **Author contributions**

472 C.C., S.G. and N. R. performed all photocatalytic experiments. S.V. synthesized and characterized czbpy
473 and poly-czbpy. S.S. and C.T carried out EPR studies. B.P., A.T. and P.H.S., directed all research efforts.
474 B.P. and A.T. conceived the research study. C.C., S.G. and B.P. wrote the manuscript with contributions
475 from all authors.

476

477 **Competing interest statement**

478 The authors declare no competing interests.

479 **Additional information**

480 A version of this research was previously posted to ChemRxiv.